NWSC/CR/RDTR-16

ALKALI METAL EMITTERS

I. Analysis of Visible Spectra

Naval Weapons Support Center
Applied Sciences Department
Crane, Indiana 47522

6 October 1975

FINAL REPORT for Period 1 July 1973 to 1 July 1975

Prepared for
Commander
Naval Air Systems Command
(Code AIR-310C)
Washington, D. C. 20361

Submitted

B. E. DOUDA, Manager
Chemical Sciences Branch
Pyrotechnics Division
Applied Sciences Department

UNCLASSIFIED

SECURITY CLASSIFICATION OF THIS PAGE (When Data Entered)

REPORT DOCUMENTATION PAGE

READ INSTRUCTIONS BEFORE COMPLETING FORM

1. REPORT NUMBER: NWSC/CR/RDTR-16	2. GOVT ACCESSION NO. / 3. RECIPIENT'S CATALOG NUMBER
4. TITLE (and Subtitle): ALKALI METAL EMITTERS. I. Analysis of Visible Spectra.	5. TYPE OF REPORT & PERIOD COVERED: Final Report. 1 Jul 73 to 1 Jul 75
	6. PERFORMING ORG. REPORT NUMBER
7. AUTHOR(s): Henry A. Webster III	8. CONTRACT OR GRANT NUMBER(s): A310310C/159A/ 5R02402002
9. PERFORMING ORGANIZATION NAME AND ADDRESS: Naval Weapons Support Center, Applied Sciences Department, Crane, Indiana 47522	10. PROGRAM ELEMENT, PROJECT, TASK AREA & WORK UNIT NUMBERS: 61153N, WR02402, WR02402002, Work Unit No. 1
11. CONTROLLING OFFICE NAME AND ADDRESS: Commander, Naval Air Systems Command (AIR-310C), Washington, D. C. 20361	12. REPORT DATE: 6 Oct 75
	13. NUMBER OF PAGES: 33
14. MONITORING AGENCY NAME & ADDRESS (if different from Controlling Office)	15. SECURITY CLASS. (of this report): Unclassified
	15a. DECLASSIFICATION/DOWNGRADING SCHEDULE

16. DISTRIBUTION STATEMENT (of this Report)

APPROVED FOR PUBLIC RELEASE; DISTRIBUTION UNLIMITED

17. DISTRIBUTION STATEMENT (of the abstract entered in Block 20, if different from Report)

18. SUPPLEMENTARY NOTES

19. KEY WORDS (Continue on reverse side if necessary and identify by block number)

Pyrotechnics, Spectroscopy, Alkali Metals, Visible Emission

20. ABSTRACT (Continue on reverse side if necessary and identify by block number)

See reverse

409 251

DD FORM 1 JAN 73 1473 EDITION OF 1 NOV 65 IS OBSOLETE S/N 0102-014-6601

UNCLASSIFIED

SECURITY CLASSIFICATION OF THIS PAGE (When Data Entered)

Visible spectra of flares containing magnesium as a fuel and lithium, sodium, potassium, rubidium and cesium nitrates as the oxidizers are presented. Atomic and molecular emissions are identified and assigned to electronic transitions. The emission characteristics of the atomic emitters are the same as those observed in other studies. Several emission bands, possibly from diatomic alkali metal species, are observed and tentatively assigned.

The intensity of the 518 nm magnesium line is seen to decrease by two orders of magnitude when the oxidizer is changed from lithium nitrate to cesium nitrate. This change could not be easily explained on the basis of calculated equilibrium temperatures and species concentration.

Recommendations for further work are discussed.

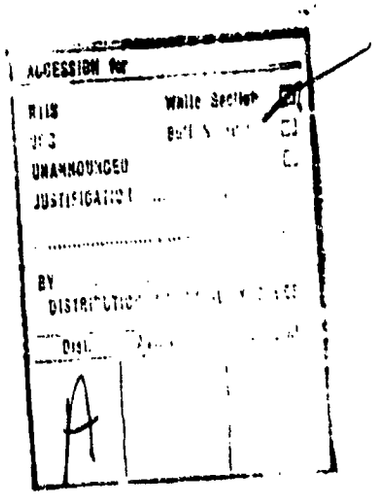

TABLE OF CONTENTS

FIGURES

TABLES

INTRODUCTION

Pyrotechnic compositions used for the production of visible light, either for illumination or for signaling purposes, rely on emission from atomic and molecular species formed as reaction products from the combustion of magnesium and a solid oxidizer, usually an alkali or alkaline earth metal nitrate or perchlorate.[1] The most widely studied system is the magnesium-sodium nitrate flare which is used for illuminating purposes. It has been shown that most of the visible light produced by this flare comes from the broadened sodium resonance lines centered at 589 nm.[2-4] During the course of the studies to determine the processes occurring in the magnesium-sodium nitrate system, additional information was obtained on the visible and near-infrared spectra of pyrotechnic compositions containing barium and strontium salts and the other alkali metal nitrates; namely, lithium, potassium, cesium and rubidium.[5,6] It was determined that the use of any alkali or alkaline earth metal nitrate other than sodium nitrate for illumination purposes was unsatisfactory. The use of alkali metal nitrates for colored signals was also considered unsatisfactory in comparison to the alkaline earth compounds currently used. It was apparently for these reasons that no attempt was made to further investigate the spectra of the magnesium/alkali metal nitrate flares in any detail. The spectra were presented as either direct reproductions of the spectrograph film[5] or rapid scanning spectrometer data.[6] In neither case was any detailed attempt made to discuss or to analyze the spectra.

Since the alkali metal nitrates and perchlorates find wide use in pyrotechnics, it appears reasonable to more completely evaluate the emission characteristics of flares containing magnesium and an alkali metal-containing species. This is the first in a series of reports which will attempt to characterize the processes occurring in flares containing lithium, sodium, potassium, rubidium and cesium nitrates as oxidizers. This first report will describe the visible emission spectra of these flares.

EXPERIMENTAL

Initial Calculations

To completely accomplish the objectives of the work, a series of experimental flares were made which were designed to allow investigations of the emission spectra of high and low concentrations of alkali metal emitters and the emission spectra of combinations of emitters. An initial series of calculations was done using the NASA thermodynamics program[7] to optimize the magnesium, alkali metal nitrate, binder formulations to give the maximum adiabatic temperature. The organic binder level was fixed at five percent and the fuel to oxidizer ratio was varied until the maximum temperature was computed. The final formulas used in this study are given in Table 1. Table 2 contains the computed maximum temperatures and the important species concentrations for the formulas. As can be seen from Table 2, the adiabatic temperatures decrease in order Li>Na>K>Rb>Cs as would be predicted.

An examination of Table 1 reveals that formulations 7307, 7308, 7312 and 7313 contain mixtures of different alkali metal nitrates. The purpose of these formulations was two-fold. The major reason for doing this was to provide high and low concentrations of the alkali metals (on the order of 100:1) for spectral measurements in the resonance line region of the spectrum. The results of this study will be published in Part III of this series of reports. The second reason was to allow an examination of the visible spectrum for possible alkali metal diatomic molecular emission.

Construction of Flares

The chemicals used in making the formulations ranged from research grade lithium, rubidium and cesium nitrate to a practical grade sodium and potassium nitrate. These oxidizers were ground and dried prior to mixing. The particle size was approximately 30 microns. The magnesium was MIL-M-382, granulation 17, which has an approximate particle size of 75 microns. The binder used was a combination of Dow Epoxy Resins®, DER 321 and DER 732 and a polyamine CX 3482.1 in the ratio DER 321 - 61.3%, DER 732 - 26.3% and CX 3482.1 - 12.4%. This is a typical epoxy binder formulation currently in use in illuminating flares. In an effort to prevent contamination, the mixing, screening and drying apparatus was washed and dried between each formula change.

TABLE 1. FLARE FORMULATIONS

Group 7307

Magnesium	43.2%
Lithium Nitrate	51.1
Rubidium Nitrate	0.7
Binder	5.0

Group 7308

Magnesium	39.6%
Sodium Nitrate	54.9
Lithium Nitrate	0.5
Binder	5.0

Group 7309

Magnesium	25.3%
Rubidium Nitrate	69.7
Binder	5.0

Group 7310

Magnesium	19.8%
Cesium Nitrate	75.2
Binder	5.0

Group 7311

Magnesium	35.2%
Potassium Nitrate	59.8
Binder	5.0

Group 7312

Magnesium	43.2%
Lithium Nitrate	51.05
Cesium Nitrate	0.75
Binder	5.0

Group 7313

Magnesium	43.2%
Lithium Nitrate	50.65
Sodium Nitrate	0.55
Potassium Nitrate	0.60
Binder	5.0

TABLE 2. CALCULATED TEMPERATURES AND CONCENTRATIONS

Group #	7307	7308	7309	7310	7311	7312	7312
Max [Metal]	Li	Na	Rb	Cs	K	Li	Li
T(°K)	3081	3073	3008	2969	3056	3083	3083
[Li]*	.130	.0012	--	--	--	.1321	.1304
[Na]	--	.1882	--	--	--	--	.0018
[K]	--	--	--	--	.1858	--	.0016
[Rb]	.0008	--	.192	--	--	--	--
[Cs]	--	--	--	.1943	--	.0009	--
[MgO]	.0569	.0550	.0352	.0269	.0489	.0579	.0581
[MgO(s)]	.3807	.3644	.3454	.3274	.3612	.3781	.3782
[Mg]	.0849	.0787	.0538	.0544	.0775	.0857	.0845

*Concentrations are given in mole fraction.

The flares were pressed into paper tubes at 10,000 pounds dead load. Fifty grams of composition were used for each candle. The finished size was 3.3 cm in diameter and 5.1 cm in length. Five grams of ignition composition were pressed on the surface of each candle.

Experimental Procedure

The flares were burned face up at a distance of 6.0 meters from the spectrographs. Visible spectra from 0.40 - 0.70 μm were recorded on a Bausch and Lomb 1.5 m grating spectrograph. This instrument has a 450 line/mm grating giving a dispersion of 15 Å /mm in the first order on the photographic film. Kodak Linagraph Shellburst film was used for recording these spectra. Spectra were also taken in the region of the resonance lines using a 1 m Spex spectrograph and Kodak I-N plates. The Spex instrument has a 1200 line/mm grating and gives a first order dispersion of 8 Å/mm. Spectra of a 200 watt quartz-iodine lamp were recorded on the same plates to provide a film response correction. In these experiments the flares were masked in such a way that the spectrographs were observing a position in the flame seven centimeters above the surface of the candle.

The spectra were scanned and digitized on an Optronics S2000 densitometer. Points were taken at approximately 0.60 nm intervals. The resulting digital output was processed by standard procedures[9] and the film density converted to radiant and luminous power readings.

RESULTS

This first set of experiments was designed only to obtain the visible spectra of flares containing magnesium, an alkali metal nitrate, and a binder. No attempt was made to measure the absolute value of radiant or luminous power. Relative powers in the visible can be obtained by integrating the spectra over all wavelengths from 0.40 - 0.70 μm. The relative radiant powers are Li Na>K Cs Rb and the ratio was 1:0.04. The burning rates on all the compositions were on the order of 0.084 cm/s.

The visible radiant power spectra obtained on the Bausch and Lomb 1.5 m spectrograph for flare groups 7307 through 7313 are shown in Figs. 1-7. Each of these spectra was selected as being

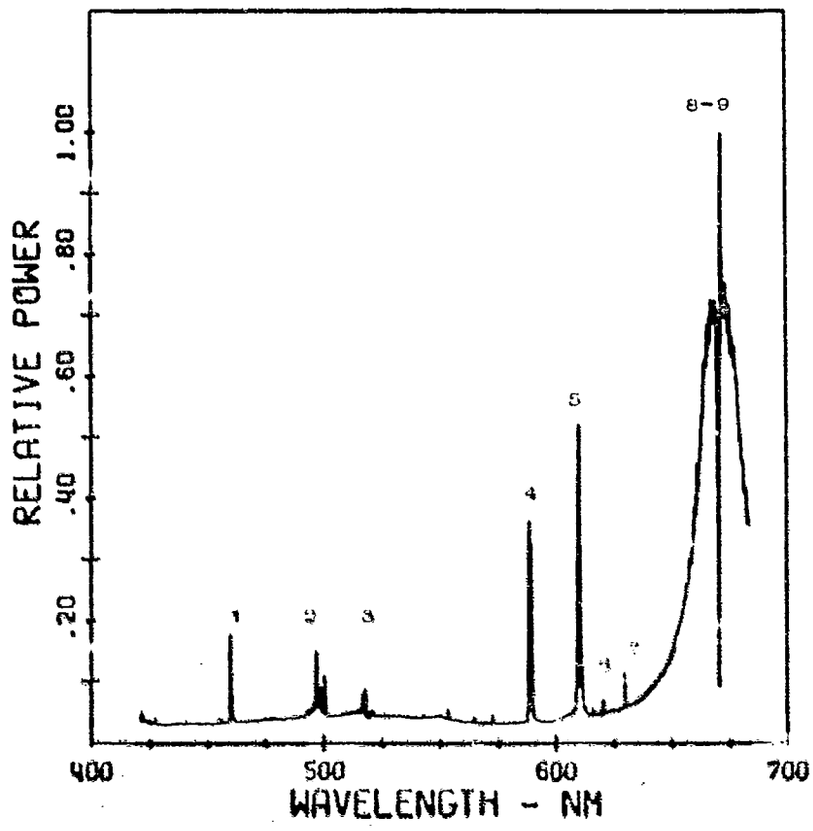

FIG. 1. Group 7307 - High [Li]/Low [Rb] - Numbered peaks correspond to following emitters and wavelengths in nm: (1) Li, 460.3, (2) MgO, 500.7, (3) Mg, 518.4, (4) Na, 589.3, (5) Li, 610.4, (6) Rb, 620.6, (7) Rb, 629.8, (8) Li, 670.8, (9) Cs, 672.4.

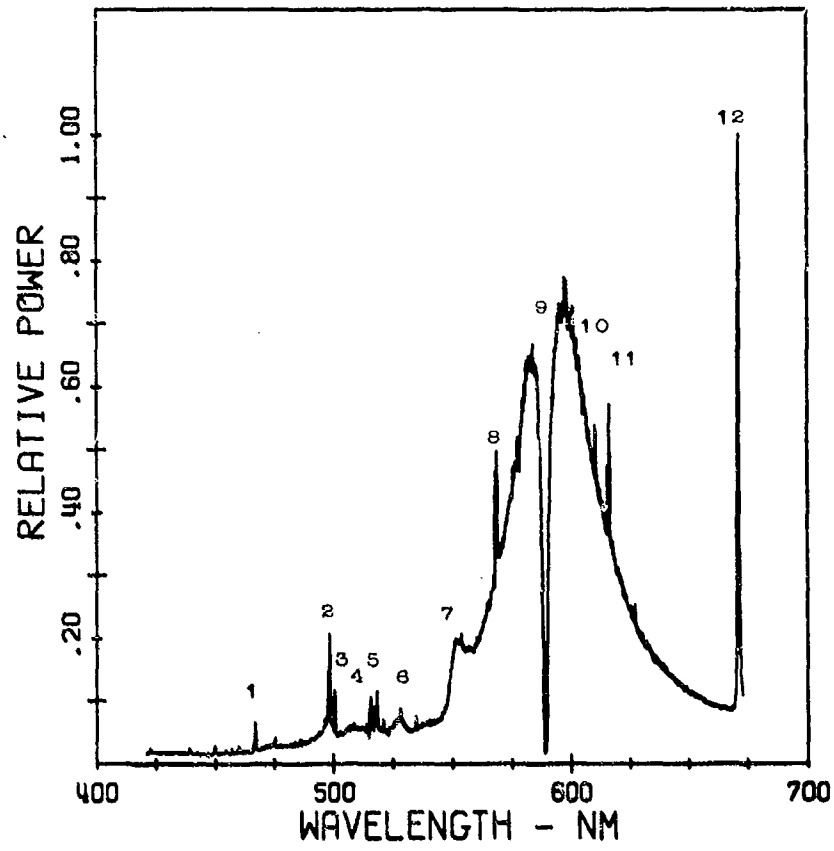

FIG. 2. Group 7308 - High [Na]/Low [Li] - Numbered peaks correspond to following emitters and wavelengths in nm: (1) Li, 460.3, (2) Na, 498.3, (3) MgO, 500.7, (4) Na, 515, (5) Mg, 518.4, (6) NaMg, 530, (7) NaN_2, 550, (8) Na, 568.5, (9) Na, 589.3, (10) Li, 610.4, (11) Na, 615.8, (12) Li, 670.8.

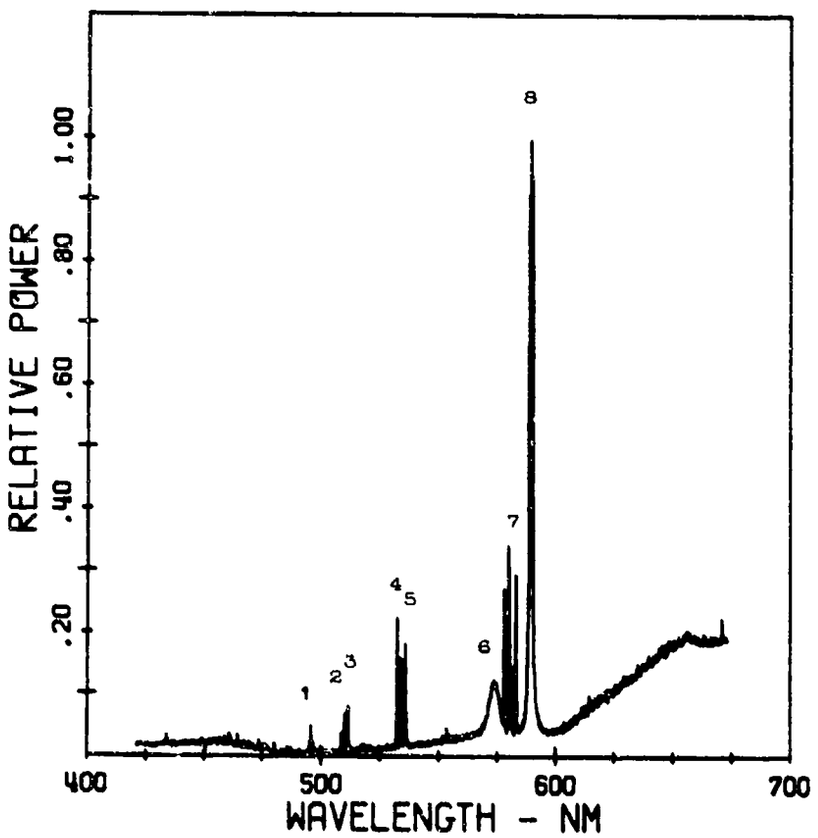

FIG. 3. Group 7311 - High [K] - Numbered peaks correspond to following emitters and wavelengths in nm: (1) K, 495.1, 495.6, 496.5, (2) K, 508.4, 509.9, (3) K, 509.7, 511.2, (4) K, 532.2, 534.0, (5) K, 534.3, 536.0, (6) K_2, 570, (7) K, 578.3, 580.2, 581.3, 583.2, (8) Na, 589.3.

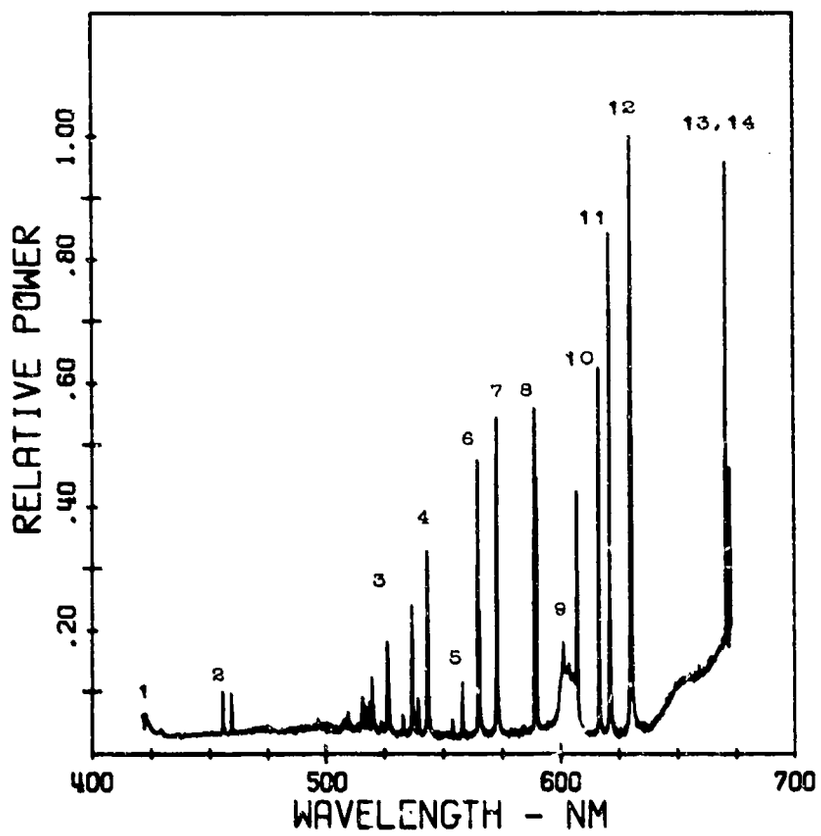

FIG. 4. Group 7309 - High [Rb] - Numbered peaks correspond to following emitters and wavelengths in nm: (1) Rb, 420.7, (2) Cs, 455.5, 459.3, (3) Unidentified, 527, (4) Rb, 539.4, (5) Rb, 557.9, (6) Rb, 564.8, (7) Rb, 572.5, (8) Na, 589.3, (9) Rb_2, 600, (10) Rb, 616.0, (11) Rb, 620.6, (12) Rb, 629.8, (13) Li, 670.8, (14) Cs, 672.4.

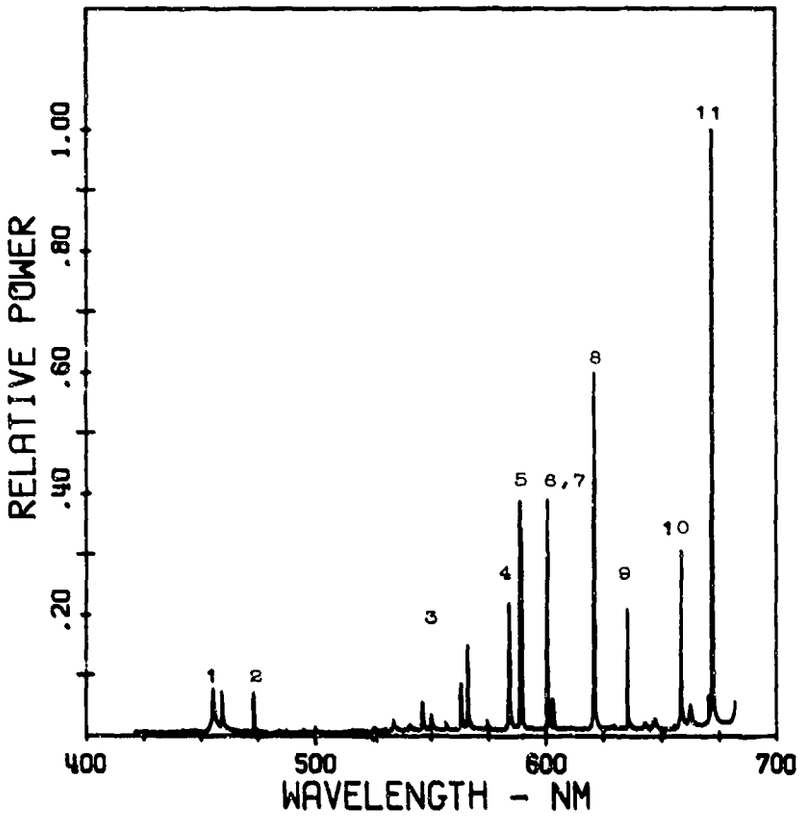

FIG. 5. Group 7310 - High [Cs] - Numbered peaks correspond to following emitters and wavelengths in nm: (1) Cs, 455.5, 459.3, (2) Cs, 473.2, (3) Unidentified, 550, (4) Cs, 584.4, (5) Na, 589.3, (6) Cs, 601.0, (7) Cs, 603.4, (8) Cs, 621.3, (9) Cs, 635.6, (10) Cs, 678.7, (11) Cs, 672.4.

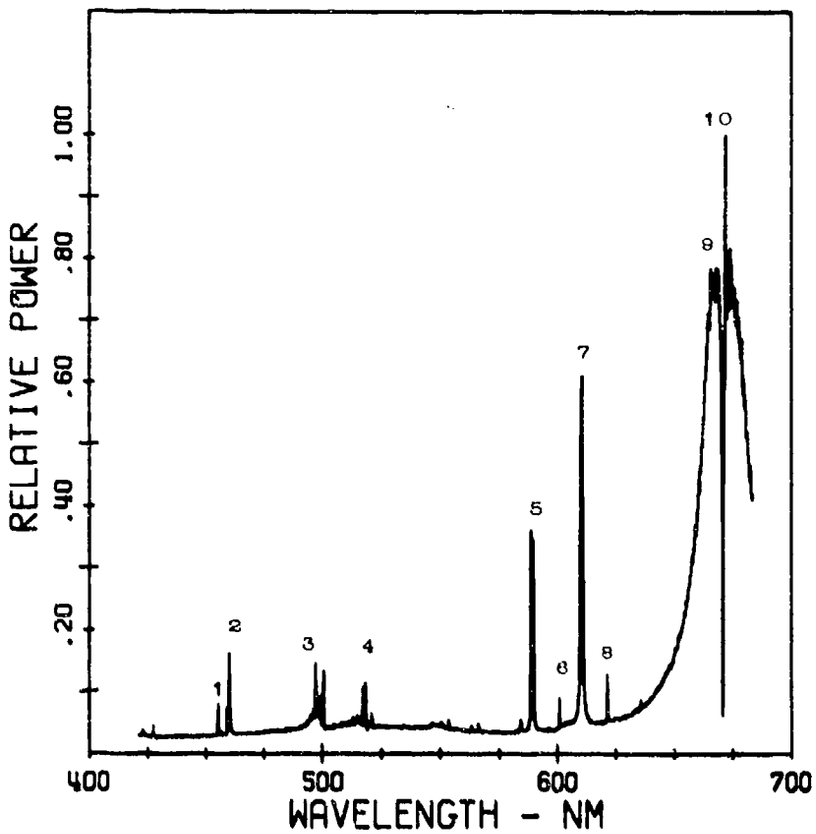

FIG. 6. Group 7312 - High [Li]/Low [Cs] - Numbered peaks correspond to following emitters and wavelengths in nm: (1) Cs, 455.5, (2) Li, 460.3, (3) MgO, 500.7, (4) Mg, 518.4, (5) Na, 589.3, (6) Cs, 601.0, (7) Li, 610.4, (8) Cs, 621.3, (9) Li, 670.8, (10) Cs, 672.4.

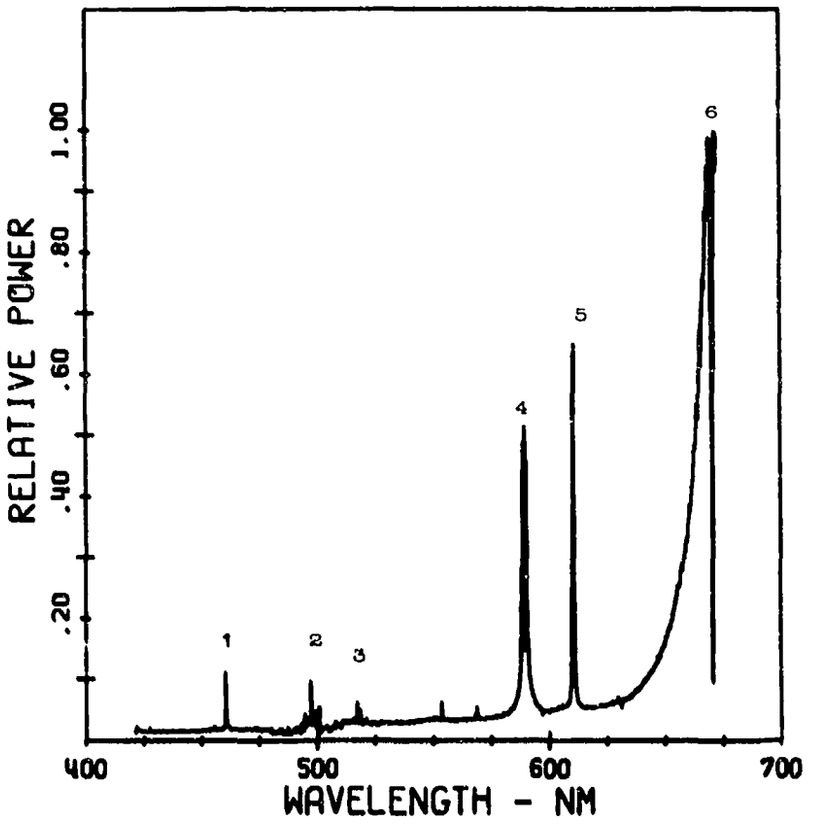

FIG. 7. Group 7313 - High [Li]/Low [Na]/Low [K] - Numbered peaks correspond to following emitters and wavelengths in nm: (1) Li, 460.3, (2) MgO, 500.7, (3) Mg, 518.4, (4) Na, 589.3, (5) Li, 610.4, (6) Li, 670.8.

representative of a large number of spectra obtained for each group. The spectral distributions are essentially unchanged within a particular formulation group. To avoid confusion and to show as much of the important structure as possible, each figure is normalized to a value of one at its maximum. The relative magnitudes of the maxima are 1.0:1.0:0.02:0.03:0.04 for Li, Na, K, Rb and Cs, respectively.

No inconsistencies with visual observations were observed. The flares containing a high lithium concentration, e.g. group 7307, appeared red to pink. Those containing high sodium appeared yellow-white. The flares with cesium and rubidium appeared white and the potassium flares tended to be purple. Visual estimations of brightness were in agreement with the relative radiant power measurements presented earlier.

DISCUSSION

Assignment of the Spectra

Lithium

The electronic structure of lithium is $1s^2 2s^1$ making the ground state a 2s. The following assignments are made for the lithium spectrum shown in Fig. 1. The flare burned to get this spectrum was formulation 7307, high lithium - low rubidium concentration. Reading from short to long wavelength, the peak at 460.29 nm is assigned to the 4d→2p transition in lithium. The next three peaks are MgO bands, B→X transition, at 498.59, 499.67 and 500.7 nm and are assigned to the 2,2; 1,1 and 0,0 transitions, respectively. Any information gained from these bands and other features associated with MgO is uncertain due to a lack of basic information regarding potential energy curves, ground state assignments, etc.[8] This region will be observed in more detail and the results given in another report. The next observable feature is the series of three lines at 516.73, 517.27 and 518.36 nm and these are assigned to the 4s→3p transition of atomic magnesium. The next major feature is the sodium resonance doublet at 589 nm. This sodium emission is strong but the sodium is present only as an impurity. The strong peak at 610.36 nm is assigned to the 3d→2p transition of atomic lithium. The two small peaks at 620 and 630 nm are rubidium and will be discussed later.

The most striking feature and the feature which contributes most of the visible energy is the broadened lithium resonance line centered at 670.78 nm, the 2p→2s transition. The broadening at half-height is slightly greater than 20 nm. A further discussion of the alkali metal resonance line broadening will be presented in another report. The sharp line located at 672.34 nm is due to a cesium impurity and its assignment will be discussed in conjunction with the cesium analysis.

There were no unexpected features observed in the magnesium-lithium nitrate flare.

Sodium

Although a great deal has been written about the sodium nitrate flare, we will analyze sodium in the same way as the other alkali metal nitrates in order to provide complete documentation. Much of what is written here is certainly redundant.

The electronic structure of sodium is $1s^2 2s^2 2p^6 3s^1$ making the ground state energy level of the sodium atom a 3s. The spectrum to be assigned is the one given in Fig. 2; the flare formula is 7308, high sodium - low lithium concentrations. The first apparent peak is the lithium peak at 460.29 nm described previously. The next series of peaks are the MgO bands at 500.7 nm. In addition, there is a sodium peak superimposed on these bands at 498.28 nm. This peak is due to the 5d→3p transition. The next two lines are the sodium doublet at 514.91 and 515.36 nm and are due to the 6s→3p transition. The next three lines are the magnesium lines at 516.73, 517.27 and 518.36 nm discussed previously. There is next an apparently continuous band-type feature at 530 nm and this will be discussed later.

The major feature in the sodium spectrum is the broadened resonance line continuum which has been well described both experimentally and theoretically by Douda.[2,3] The emission is centered at 589.3 nm and is due to the 3p→3s transition. The halfwidth of the broadened lines is approximately 50 nm.

Superimposed on the short wavelength side of the continuum is a sodium doublet at 568.27 and 568.82 nm. These lines are due to the 4d→3p transition. Superimposed on the long wavelength side are the lithium lines at 610.36 nm and 670.79 nm and another sodium doublet at 615.42 and 616.07 nm due to the 5s→3p transition.

Returning to the band feature at 530 nm, we will make tentative assignments only as to possible molecular emitters and delay any detailed discussion to the second report in this series. The emission at 530 nm appears to be completely continuous and has previously been assigned to a NaMg molecular interaction.[10] The "shoulder" which

appears at 550 nm on the wing of the broadened sodium resonance line has been assigned both to a sodium-nitrogen satellite interaction and to diatomic sodium.[6,11] The actual assignment remains in question and will be discussed at length in the next report.

Potassium

Potassium salts find heavy use in pyrotechnics as oxidizers probably because of their relative inexpensiveness and lack of emission in the visible spectral region. The fact that potassium does have significant visible emission may account in part for the current inability to obtain high purity colors in signals which incorporate it as an oxidizer.

The electronic structure of potassium is $1s^2 2s^2 2p^6 3s^2 3p^6 4s^1$ making its ground electronic state a 4s. The assignments are made for Fig. 3, flare formula 7311, consisting of magnesium, potassium nitrate and binder only. In terms of specific line emission, the potassium spectrum is relatively simple. Barely distinguishable at approximately 490 nm are three potassium lines assigned as 495.08, 495.60 and 496.50 nm. These lines are a result of the transitions 8d→4p, 10s→4p and 8d→4p. The next series of lines are two doublets at 508.42, 509.92, 509.71 and 511.20 nm and are assigned to the transitions 9s→4p and 7d→4p. Two more potassium doublets are observed at 532.23, 533.97 and 534.30, 535.95 nm and are due to the 8s→4p and 6d→4p transitions. A fourth set of potassium doublets is observed at 578.26, 580.20 and 581.25, 583.21 nm and are assigned to the 7s→4p and 5d→4p transition. The sodium doublet at 589 nm is due to an impurity in the mix. Quantitative analysis of a similar composition showed the concentration of the sodium impurity to be less than 1 ppm. This illustrates the excellent emission properties of atomic sodium. It is possible that some of this emission comes from the paper tube. Similar work using slightly different formulas showed no reduction of the sodium emission when burned without tubes[12] so the case is probably not the origin of the emission.

There are several features in the potassium spectra which warrant attention. The first feature is the symmetrical hump centered at 570 nm. This continuous feature is tentatively assigned to diatomic potassium and will be discussed in greater detail in the next report. Another feature is the sharply increasing continuum starting at 600 nm and continuing outward. The leveling off of this feature at 650 nm may or may not be real since in this region both the film and spectrograph are rapidly losing response and the apparent leveling may be an artifact of this loss in sensitivity. No assignment has been made at this time. It is possible that this feature is the tail of the broadened potassium resonance line continuum centered at 768.2 nm. However, the broadening in potassium would have to be excessively

large for this to be the case. Similarly the increased continuum observed at 425-475 nm might also be due to broadening of the 404.5 doublet in potassium, the other transition, 5p→4s, going to the ground state. As more data is reduced, the origins of these continuous emissions may become more apparent. These also will be discussed in the next report. There are observed transitions in diatomic potassium at 650 nm and at 406 nm.[9] These have been observed in absorption only.

In regard to missing features, it is interesting to note the apparent absence of the Mg and MgO emissions. These emissions actually are present. However, on the scale used in this figure, they are too small to be seen. As can be seen from Table 2, this might be due to a loss in the temperature of the system. If this is the case, conceivably the magnesium lines and the MgO band system could be used as a guide to determining the temperature distribution in a pyrotechnic flame. This will be discussed in more detail in another section of this report.

Rubidium

The electronic structure of rubidium is $1s^2 2s^2 2p^6 3s^2 3p^6 3d^{10} 4s^2 4p^6 5s^1$ making the ground state a 5s. The assignments given are for Fig. 4, flare formula 7309, consisting of magnesium, rubidium nitrate and binder. As can be seen from Fig. 4, rubidium has a large number of emission lines in the visible. At the extreme left of the figure, centered at 420.7 nm, we see the 6p→5s transition in rubidium. Unfortunately the sensitivity of the film was such that this feature was barely apparent. The two lines at 455.5 and 459.3 nm are due to a cesium impurity. In the region from 500-535 nm there are a series of several lines as yet unidentified. These are apparently narrow with little or no degrading indicating that this is probably atomic emission rather than molecular band emission. The exact wavelengths of the major lines are 515.3, 518.6, 526.4 and 532.6 nm. These lines are followed by another unidentified line at 539.4 nm.

The next line is a rubidium line at 543.15 nm and is due to the 8d→5p transition. The next rubidium line is seen at 557.88 nm and is the transition 9s→5p. The next line is actually two unresolved rubidium lines at 564.81 and 565.37 nm coming from the 7d→5p and 9s→5p transitions. Next is a rubidium line at 572.45 nm and is from the 7d→5p transition. The next line is the sodium doublet at 589 nm. Skipping the band emission at 600 nm the next line is a rubidium line at 615.96 nm arising from the 8s→5p transition. The next line is at 620.63 nm, a rubidium line from the 6d→5p transition followed by the rubidium transition at 629.83 nm. This transition is also the 6d→5p. The last two lines superimposed on a continuum are lithium at 670.7 and cesium at 672.3 nm.

The continuous emission at 600 nm, which may be molecular band emission, could be due to either diatomic rubidium or some other rubidium interaction. Further data reduction is underway and this, like the other apparent molecular species, will be discussed in the second report. The continuous emission beginning at 630 nm and continuing to cut off looks suspiciously similar to the continuum in potassium. This may be a molecular interaction, it may be only the wing of the broadened resonance line centered at 792 nm, or it may be an artifact of the spectrograph response. Further examination of the data will be presented in the second report.

Again, in this spectrum, one should note the apparent absence of the Mg and MgO emission. As in the case of potassium, the emission is present but very weak.

Cesium

The electronic structure of cesium is $1s^2 2s^2 2p^6 3s^2 3p^6 3d^{10} 4s^2 4p^6 4d^{10} 5s^2 5p^6 6s^1$ making its ground electronic state a 6s. The following assignments are for Fig. 5, flare formulation 7310, composed of magnesium, cesium nitrate and binder. The two peaks at 455.54 and 459.32 nm are cesium emission lines and are assigned to the transition 7p→6s, a transition to the ground state. Visual examination of the spectrograph film shows that these lines are reversed as one would expect. The peak at 473.2 nm as well as those at 534.2, 546.5, 550.2, 563.5 and 566.3 nm are unidentified at this time. The possibility that they are molecular emissions exists but the shapes of the lines indicate that they are probably higher level atomic cesium transitions. The next line is cesium at 584.47 nm and is due to the transition 9d→6p. The next line is the sodium doublet at 589 nm. Next is a cesium line at 601.03 nm and is the 8d→6p transition. The small line is cesium at 603.41 nm and is due to a 10s→6p transition. The next line is at 621.29 nm and is the 8d→6p cesium transition. The next line is a cesium line at 635.6 nm and is due to the 9s→6p transition. This is followed by a line at 658.65 nm and is the cesium 9s→6p transition. The final line is a strong cesium line at 672.33 nm resulting from the transition 7d→6p.

In the cesium spectra, there are no unidentified band structures or continua. As a matter of note, the Mg and MgO emissions are present but weak and the underlying graybody continuum which normally has at least a tendency to increase at the longer wavelengths is absent. It should also be noted that there is no sharply increasing emission at the extreme red end of the spectrum as was observed in both potassium and rubidium.

Mixtures

Figures 6 and 7 are the visible spectra of formula groups 7312 and 7313. Group 7312 is a high lithium - low cesium concentration formula. Group 7313 has a high lithium concentration and low sodium and potassium concentrations.

The emission features in both Figs. 6 and 7 are characteristic of lithium. The major lines are at 460.3, 610.4 and 670.8 nm. In addition, both spectra show the sodium resonance doublet at 589 nm. One should note that in Fig. 6 the sodium is present as an impurity and there is little broadening of the emission lines while in Fig. 7 the sodium concentration is about 0.2 percent and the broadening is already apparent.

In Fig. 6, the other spectral features are the Mg and MgO lines and bands and the more intense cesium emission lines. In Fig. 7, the Mg and MgO emissions are prominent features. However, the emissions from the low concentration potassium present are too weak to be shown on the scale of this figure.

It should be noted that there are no molecular emissions from diatomic or polyatomic species which might have been formed as a result of interactions between the alkali metals.

Summary

In an effort to summarize this mass of information and make it more useful, the wavelength and assigned transitions for the alkali metal nitrates only are tabulated in Tables 3 to 7. If these tables are compared to the arc emission spectra of atomic alkali metals generally tabulated,[13] one finds virtually complete agreement in both line assignments and intensities.

Disappearance of Prominent Features

As one observes the spectra in Figs. 1 to 7, it is apparent that as the alkali metal nitrates are changed from lithium to cesium, i.e., as the molecular weight of the oxidizer increases, the intensity of emission from the magnesium lines at 516.73, 517.27 and 518.36 nm and magnesium oxide bands at 500 nm decreases. This decrease is even greater than is apparent from the spectra since, for the sake of comparison, the powers have been normalized to a value of one at the maximum. At first glance this decrease could be attributed to a decrease in the temperature of the reaction. In an effort to correlate these two factors a simple calculation was made using the

TABLE 3. ASSIGNMENT OF LITHIUM LINES

Wavelength (nm)	Transition
460.29	4d→2p
497.20	4s→2p
610.36	3d→2p
670.78	2p→2s

TABLE 4. ASSIGNMENT OF SODIUM LINES

Wavelength (nm)		Transition
498.28		5s→3p
514.91		6s→3p
515.36		6s→3p
568.27		4d→3p
568.82		4d→3p
589.00	reversed and broadened	3p→3s
589.95		3p→3s
615.42		5s→3p
616.02		5s→3p

TABLE 5. ASSIGNMENT OF POTASSIUM LINES

Wavelength (nm)	Transition
495.08	8d→4p
495.60	10s→4p
496.50	8d→4p
508.42	9s→4p
509.71	7d→4p
509.92	9s→4p
511.20	7d→4p
532.23	8s→4p
533.97	8s→4p
534.30	6d→4p
535.95	6d→4p
578.26	7s→4p
580.20	7s→4p
581.25	5d→4p
583.21	5d→4p

TABLE 6. ASSIGNMENT OF RUBIDIUM LINES

Wavelength (nm)		Transition
420.70	reversed	6p→5s
536.26		8d→5p
543.15		8d→5p
557.88		9s→5p
564.81		7d→5p
565.37		9s→5p
572.45		7d→5p
615.96		8s→5p
620.63		6d→5p
629.83		6d→5p

TABLE 7. ASSIGNMENT OF CESIUM LINES

Wavelength (nm)		Transition
455.54	reversed	7p→6s
459.32	reversed	7p→6s
584.47		9d→6p
601.03		8d→6p
603.41		10s→6p
621.29		8d→6p
635.60		9s→6p
658.65		9s→6p
672.33		7d→6p

Boltzmann equation to calculate the population of the upper levels which give rise to these transitions. We know that the intensity of an atomic line in emission is given by

$$I_{em}^{nm} = N_n h c \nu_{nm} A_{nm} \qquad (1)$$

where N_n is the population in the n^{th} level, A_{nm} is the fraction of atoms carrying out the transition from level n to level m per second and $hc\nu_{nm}$ is the energy of a light quantum of wavenumber ν_{nm}.[9] In the calculation to be done, we will consider only a single emission line, the magnesium line at 518.36 nm. Thus, in Eqn. (1), the only quantity which changes as we change the oxidizer in the system is the population of the upper level, level n. The concentration in the upper level is given by the Boltzmann equation,

$$N_n = N_{tot} e^{-E/kT} \qquad (2)$$

where N_{tot} is the concentration of the magnesium, E is the energy associated with the 518.36 nm wavelength, k is Planck's constant and T is the temperature of the system. The results of this calculation for the systems under consideration are given in Table 8. In this table the experimentally obtained intensity of the magnesium line, I(Mg), at 518.36 nm is given relative to its maximum value, i.e., the value when lithium nitrate is used as the oxidizer. Since lithium nitrate was used in several formulas as the main oxidizer, there was a chance for comparison of the intensity of the magnesium line for precision among different spectra. For all systems chosen and for several spectra in each system exposed for different times, the agreement among the magnesium intensities was ±20%. While this error is not small enough to allow for quantitative discussions of populations, it is sufficiently accurate to allow a general comparison between what is predicted by theory and what is observed experimentally. The values for the magnesium concentration, [Mg], again relative to the value when the oxidizer is lithium nitrate, and the temperatures, T, given in Table 8 were obtained from the thermodynamic calculations given in Table 2. The quantity N_n is the relative population of the excited state of magnesium and is obtained by multiplying the concentration of magnesium by the Boltzmann factor at the specified temperature. Examination of Table 8 reveals that the theoretical change in the upper state concentration, N_n, is only a factor of about two while the observed change in intensity, I(Mg), is over a factor of 100. Obviously then there are additional factors which one must consider in order to treat this problem.

TABLE 8. INTENSITY AND CALCULATED POPULATION FOR MAGNESIUM

Molecular Species	Group #	T°K	Boltzmann Factor	[Mg]	N_n	I(Mg)*
Li	7313	3083	1.0	1.0	1.0	1.0
Na	7308	3073	0.97	0.93	0.90	0.50
K	7311	3056	0.92	0.91	0.84	0.038
Rb	7309	3008	0.80	0.64	0.51	0.010
Cs	7310	2969	0.71	0.64	0.45	0.009

*Determined experimentally. All other quantities in this Table are calculated.

The experiments performed here were not in any way designed to explain this phenomena. A detailed analysis of the observed decrease in intensity is not only beyond the scope of this paper but is probably impossible due to a lack of the necessary information. Any efforts to resolve this problem will have to be undertaken with entirely different methods and procedures.

The most likely explanation for the observed decreases lies not only in a discussion of temperature and concentration but also in a discussion of the distribution of the available energy released by the chemical reactions. Thermodynamic calculations have shown that the energy available from these reactions are 1.93, 1.47, 1.20 and 0.64 kcal/g for lithium, sodium, potassium and cesium nitrate reacting with magnesium, respectively.[14] This calculation assumed that the reaction products were at 1200°K. The reasoning behind this assumption and a method for using these numbers to obtain total luminous power has been presented earlier.[15] Unfortunately for purposes of this discussion total luminous power has no significance. It should also be noted that the energies presented above are for slightly different formulas; however, the trend will be the same.

As can be seen, there is significantly less energy available in the higher molecular weight nitrates. If this energy is now distributed differently among the various atomic levels, the observed factor of 100 decrease in intensity could probably be explained. For example, if in the case of cesium nitrate, significantly more of the energy were contained in the resonance line continuum, there would be less available for populating the upper states of magnesium and magnesium oxide and the observed decrease might easily be predicted. Any more detailed analysis than this simple "handwaving" argument will be delayed until more accurate data is obtained on the distribution of energy in the products of the reactions.

Other factors which might affect the ability to predict the observed decrease in intensity include (a) the inability of thermodynamics alone to predict species concentration and reaction kinetics in the system, (b) the lack of sufficient information concerning quenching processes which occur, and (c) the problem associated with observing emitting species in a region of the flame where their concentration is low and their emission not its maximum. As was pointed out previously, since these experiments were not designed to answer any of these questions, further discussion is merely speculation and will not be pursued at this time.

An understanding of these problems is definitely needed. For example, one might be attempting to make a flare that produced significant infrared radiation while minimizing the visible radiation. If one could choose additives which would decompose to form products

which would accept some or all of the excess energy of the reaction it should be possible to quench the visible emission. If these compounds could also be chosen so that their products emitted infrared radiation or transferred the energy to an infrared emitter, one would not only have eliminated the visible radiation but would also have increased the power of the infrared radiation given off.

CONCLUSIONS AND RECOMMENDATIONS

The purpose of this work was to identify and characterize the emission from flares containing magnesium as a fuel and the various alkali metal nitrates as oxidizers. The emission characteristics of the atomic emitters are the same as those predicted by other studies. There were no anamolous effects observed. All the predicted lines were present and no new atomic transitions were identified.

Several molecular emission bands associated with alkali metal species were observed in flares which contained sodium nitrate, potassium nitrate and rubidium nitrate. These bands were tentatively assigned and further discussion was delayed to a second report.

A surprisingly marked effect was observed in the emission from atomic magnesium and magnesium oxide as the oxidizer was changed. The emission intensity from a magnesium line at 518.36 nm decreased by two orders of magnitude when the oxidizer species was changed from lithium nitrate to cesium nitrate. This change could not be easily explained on the basis of calculated temperature and species concentration.

On the basis of this work, the following recommendations for future work can be made:

1. To add to the current knowledge of spectroscopic and molecular data, high resolution spectra of magnesium-sodium nitrate flares should be taken in the region of the magnesium oxide $B \rightarrow X$ transition. This data would provide information about lifetimes and potential energy surfaces which is not well established.

2. Information should be obtained about the distribution of energy among the various emitters possible in a pyrotechnic flame. This work would require simultaneous spectral power measurements in all regions of the spectrum from the near ultraviolet to the middle infrared. This data would allow more refined flare formulations for producing maximum infrared power, possibly in regions as far as five micrometers. The current work appears to indicate the possibility of non-thermal energy distributions, particularly in the near-infrared region of the spectrum. If the distributions are non-thermal, then new emitting species might be added to flames which would absorb the energy now emitted in the visible and re-emit this energy in the infrared, thus increasing infrared powers.

3. Information should be obtained on species concentration in the flame to provide a better understanding of predicted flare performance. The sharp, relatively uncomplicated, magnesium and magnesium oxide lines and bands would probably be an ideal choice for making concentration measurements for comparison with calculated concentrations. At the present time, we simply assume that the thermodynamics are accurate. The results of this study tend to indicate that this might not be the case and closer examinations appear to be indicated.

REFERENCES

1. H. Ellern, *Military and Civilian Pyrotechnics* (Chemical Publishing Company, New York, 1968), p. 337.

2. B. E. Douda, *Radiative Transfer Model of a Pyrotechnic Flame*, RDTR No. 258, Naval Ammunition Depot, Crane, Indiana (1973). Available DDC-AD No. 769 273.*

3. B. E. Douda and E. J. Bair, J. Opt. Soc. Am. 60, 1257 (1970).

4. B. E. Douda and E. J. Bair, J. Quant. Spectrosc. Radiat. Transfer, 14, 1091 (1974).

5. B. E. Douda, R. M. Blunt and E. J. Bair, J. Opt. Soc. Am. 60, 1116 (1970).

6. R. M. Blunt, *Study of Illuminating Flames from Solid Reactants*, RDTR No. 77, Naval Ammunition Depot, Crane, Indiana (1970). Available DDC-AD No. 707 720.

7. S. Gordon and B. J. McBride, *Computer Program for Calculation of Complex Chemical Equilibrium Compositions, Rocket Performance, Incident and Reflected Shocks, and Chapman-Jouguet Detonations*, NASA SP-273, Lewis Research Center (1971). Available NTIS-N71 37775.**

---

* Available DDC indicates that this document is available from Defense Documentation Center, Cameron Station, Alexandria, Virginia 22314.

** Available NTIS indicates that this document is available from National Technical Information Service, 5285 Port Royal Road, Springfield, Virginia 22161.

8. H. A. Webster and C. W. Gilliam, *Spectral Characteristics of Flares Containing Sodium Iodate as an Oxidizer*, RDTR No. 276, Naval Ammunition Depot, Crane, Indiana (April 1974). Available DDC-AD No. 782 510.

9. G. Herzberg, *Spectra of Diatomic Molecules* (D. Van Nostrand Co., Inc., Princeton, N. J., 1966).

10. D. R. Dillehay, *Possible Mechanisms for Burning Rate/Candlepower Enhancement of Illuminants* in *Proceedings - Third International Pyrotechnics Seminar* held at Colorado Springs, Colorado, 21-25 August 1972. (Sponsored by Denver Research Institute, University of Denver), p. 1. Available DDC-AD No. 913 408L.

11. R. M. Blunt, *Spectral Distribution of Different Regions in Illuminating Flare Flames II*, RDTR No. 292, Naval Ammunition Depot, Crane, Indiana (January 1975). AD-A004618

12. C. E. Dinerman and H. A. Webster, *Alkali Metal Nitrate Oxidizers for IR Illumination.* (To be published)

13. A. R. Striganov and N. S. Sventitskii, *Tables of Spectral Lines of Neutral and Ionized Atoms* (Plenum Data Corporation, New York, N. Y., 1968).

14. J. E. Tanner, Jr., *Thermodynamics of Combustion of Various Pyrotechnic Compounds*, RDTR No. 277, Naval Ammunition Depot Crane, Indiana (June 1974). Available DDC-AD No. 786 216.

15. H. A. Webster, J. E. Tanner, Jr., and B. E. Douda, *Theoretical Light Yields from Different Illuminating Flare Compositions*, RDTR No. 253, Naval Ammunition Depot, Crane, Indiana (June 1973). Available DDC-AD No. 767 928.

DISTRIBUTION LIST

ADDRESS	COPIES
Commander Naval Air Systems Command Department of the Navy Washington, D. C. 20361	
Attention: Code AIR-954, Technical Library	1
Code AIR-53235, Mr. R. Szypulski	1
Code AIR-350, Mr. E. Fisher	1
Code AIR-350E, Mr. J. Lee	1
Code AIR-310C, Dr. H. Rosenwasser	1
Commander Naval Sea Systems Command Naval Sea Systems Command Headquarters Washington, D. C. 20362	
Attention: Code SEA-09G3, Technical Library	1
Code SEA-033, CDR J. R. Gauthey	1
Code SEA-0332, Dr. A. B. Amster	1
Code SEA-9921, CDR R. Hoyt	1
Code SEA-9921B, Mr. W. Greenlees	1
Code SEA-03415, Mr. T. Tasaka	1
Administrator Defense Documentation Center for Scientific and Technical Information (DDC) Building 5, Cameron Station Alexandria, Virginia 22314	12
Commander Naval Weapons Center China Lake, California 93555	
Attention: Code 4543, Mr. J. Ramnarace	1
Code 6082, Mr. J. Eisel	1
Code 533, Technical Library	1
Code 454, Mr. Duane Williams	1
Code 45403, Dr. R. Reed	1
Code 4544, Dr. M. Nadler	1
Commander Air Force Avionics Laboratory Wright-Patterson Air Force Base Ohio 45433	
Attention: Code AFAL/CC	1
Code AFAL/WRD-2, Mr. G. Schively	1
Code AFAL/WRW-3, Mr. F. D. Linton	1
Dr. John E. MacAulay	1

DISTRIBUTION LIST (CONT.)

ADDRESS	COPIES
Commander Wright-Patterson Air Force Base Ohio 45433 Attention: Code 2750/SSL, Technical Library	1
Commander Aeronautical Systems Division (AFSC) Wright-Patterson Air Force Base Ohio 45433 Attention: Code ASD/ENAMA, Mr. M. Edelman Code ASD/ENADC, Mr. R. Sorenson Code ASD/RWE, Mr. H. Wigdahl	 1 1 1
Commander Aerospace Research Laboratory Wright-Patterson Air Force Base Ohio 45433 Attention: Code ARL(LJ), Mr. R. Tischer	 1
Commander Naval Surface Weapons Center White Oak Laboratory Silver Spring, Maryland 20910 Attention: Code 231 Technical Library	 1 1
Commanding Officer Picatinny Arsenal Dover, New Jersey 07801 Attention: Code SARPA-FR-E-L, Mr. T. Boxer Code SARPA-FR-E-L-C, Dr. F. Taylor Code SARPA-TS-S, Technical Library	 1 1 1
Commander Armament Development and Test Center Eglin Air Force Base Florida 32542 Attention: Code ADTC/SDWM, Mr. C. Lutz Code ADTC/SDWE, Mr. S. Lander	 1 1
Commander Air Force Armament Laboratory Eglin Air Force Base Florida 32542 Attention: Code AFATL/DLJW, Mr. A. Beach Code AFATL/DLMQ-3, Dr. D. B. Ebeoglu Code AFATL/DLMI, Dr. P. M. Collins Code AFATL/DLJM, Mr. D. J. Edwards	 1 1 1 1

DISTRIBUTION LIST (CONT.)

ADDRESS	COPIES
Commander Army Systems Command Development Division St. Louis, Missouri 62166 Attention: Code AMSAV-EX, Ms. M. Meyer	1
Commanding General U.S. Army Tank Automotive Command Warren, Michigan 48090 Attention: Code AMSTA-RHFL	1
Commanding Officer Naval Avionics Facility Indianapolis, Indiana 46218 Attention: PC-004, Mr. P. Collignon	1
Commander Naval Surface Weapons Center White Oak Laboratory Silver Spring, Maryland 20910 Attention: Code 250, Dr. W. McQuistion Code 252, Dr. T. Austin Code 423, Mr. F. Browning	1 1 1
Commander Naval Surface Weapons Center Dahlgren Laboratory Dahlgren, Virginia 22448 Attention: Code DG-30, Mr. R. Morrissette	1
Commanding Officer Frankford Arsenal Philadelphia, Pennsylvania 19173 Attention: Code SARFA-NOP-Y, Mr. W. Puchalski	1
Commander Edgewood Arsenal Aberdeen Proving Ground, Maryland 21010 Attention: Code SAREA-DE-NNP, Mr. M. Penn	1
Commander Ballistic Research Laboratories Interior Ballistics Laboratory Aberdeen Proving Ground, Maryland 21005 Attention: Code AMXBR-IB, Mr. J. R. Ward	1

DISTRIBUTION LIST (CONT.)

ADDRESS	COPIES
Director Naval Research Laboratory Department of the Navy Washington, D. C. 20375	
Attention: Code 5309, Mr. C. M. Loughmiller	1
Code 5500, Dr. J. M. MacCallum, Jr.	1
Commanding Officer Naval Missile Center Point Mugu, California 93042	
Attention: Code 1251(N351), Mr. N. M. Uros	1
Code 5353, Mr. D. T. Stowell	1
Commander Naval Ordnance Station Indian Head, Maryland 20640	
Attention: Code 5033K, Mr. W. Vreatt	1
Commanding General U.S. Army Missile Command Redstone Arsenal Alabama 35809	
Attention: Code AMSMI-REI, Mr. W. Hyman	1
Code AMSMI-REI, Mr. T. Jackson	1
Commander U.S. Army Material Systems Analysis Agency Aberdeen Proving Ground Maryland 21005	
Attention: Code AMX-SY-RE, Mr. J. Sheldon	1
Code AMX-SY-T, Mr. P. Topper	1
Commander Rome Air Development Center Griffiss Air Force Base New York 13441	
Attention: Code IRAD	1
The Johns Hopkins University Applied Physics Laboratory 8621 Georgia Avenue Silver Spring, Maryland 20910	
Attention: Library Acquisitions, Bldg. 5, Rm. 26	1

DISTRIBUTION LIST (CONT.)

ADDRESS	COPIES
Environmental Research Institute of Michigan P.O. Box 618 Ann Arbor, Michigan 48107 Attention: IRIA Library	1
Battelle Memorial Institute TACTEC Columbus, Ohio 43201 Attention: Ms. Nancy Hall	1
Indiana University Chemistry Department Bloomington, Indiana 47041 Attention: Dr. Edward J. Bair	1
Denver Research Institute Laboratories for Applied Mechanics University of Denver Denver, Colorado 80210 Attention: Mr. R. M. Blunt	1